DEPENDENCY OF SINGLE-PHASE FAC OF CARBON AND LOW-ALLOY STEELS FOR NPP SYSTEM PIPING ON PH, ORIFICE DISTANCE AND MATERIAL

JEONG HO MOON, HUNG HO CHUNG, KI WOUNG SUNG*, UH CHUL KIM and JAE SEONG RHO[1]
Korea Atomic Energy Research Institute
150 Deokjin-dong, Yuseong-gu, Daejeon 305-353, Korea
[1]Chungnam National University
220 Gung-dong, Yuseong-gu, Daejeon 305-764, Korea
*Corresponding author. E-mail : kwsung@kaeri.re.kr

Received December 27, 2004
Accepted for Publication May 31, 2005

To investigate the flow-accelerated corrosion (FAC) dependency of carbon steel (A106 Gr. B) and low-alloy steels (1Cr-½Mo, 2¼Cr-1Mo) on pH, orifice distance, and material, experiments were carried out. These experiments were performed using a flow velocity of 4 m/sec (partly 9 m/sec) at pH 8.0~10.0 in an oxygen-free aqueous solution re-circulated in an Erosion-Corrosion Test Loop at 130°... for 500 hours. The weight loss of the carbon steel specimens appeared to be positively dependent on the flow velocity. That of the carbon and low-alloy steel specimens also showed to be distinguishably dependent on the pH. At pH levels of 8.0~9.5 it decreased, but increased from 9.5 to 10.0. Utility water chemistry personnel should carefully consider this kind of pH dependency to control the water system pH to mitigate FAC of the piping system material. The weight loss of the specimens located further from the orifice in the distance range of 6.8~27.2 mm was shown to be greater, except for 2¼Cr-1Mo, which showed no orifice distance dependency. Low alloy steel specimens exhibited a factor of two times better resistance to FAC than that of the carbon steel. Based on this kind of FAC dependency of the carbon and low-alloy steels on the orifice distance and material, we conclude that it is necessary to alternate the composition of the secondary piping system material of NPPs, using low-alloy steels, such as 2¼Cr-1Mo, particularly when the system piping has to be replaced.

KEYWORDS : Dlow-Accelerated Corrosion, Carbon Steel, Low-Alloy Steels, Weight Loss, Dependencies

1. INTRODUCTION

Since the major rupture at Trojan in 1985, about 270 wall-thinning records for pressurized water reactors (PWRs) and about 115 records for boiling water reactors (BWRs) have been reported, as of 1995, as shown in Fig. 1 [1]. The inspections triggered by the failure that occurred at the Surry Unit 2 in 1986 have revealed numerous instances of significant erosion-corrosion at other U.S. reactors, primarily in wet-steam lines, but also in some single-phase lines. German data files for the period 1961 to 1976 showed that one-third of the 96 cases reported were for single-phase conditions [2]. A pipe rupture even occurred in 2004, as shown in Fig. 2 [3].

Wall thinning is generally caused by a flow-accelerated corrosion (FAC) and leads to a rupture with no warning unless it is detected and repaired in a timely manner. Flow-accelerated corrosion is an acceleration or increase in the rate of the corrosion caused by the relative movement between a corrosive fluid and a metal surface.

The root cause of the FAC process is the dissolution of the normally protective oxide layer from the metal surface, which leads to a local thinning of the oxide and a subsequent increase in the corrosion rates, resulting from a rapid diffusion through the oxide film [4].

Factors influencing FAC include flow velocity, steam quality, flow path geometry, water chemistry and pH, alloy content, and temperature [5-8].

Temperature is a major variable affecting the resistance to either FAC or erosion-corrosion of carbon and low alloy steels.

Most of the reported cases of FAC damage under single-phase conditions have occurred within the temperature range of 80 to 230°C The highest amount of carbon steel FAC under single-phase conditions usually occurs at 130° C, particularly in an oxygen-free aqueous solution [2, 9-10].

On the other hand, pH control is also an important factor, and many experiments have revealed the dependency

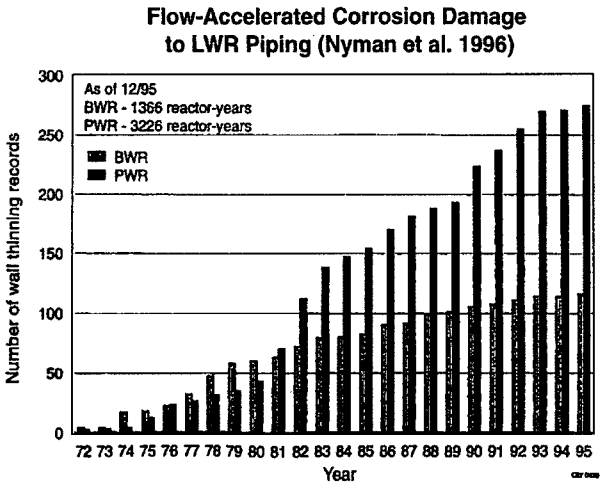

Fig. 1. World-wide Experience of the Flow Accelerated Corrosion Damage to LWR Secondary-side Piping [1]

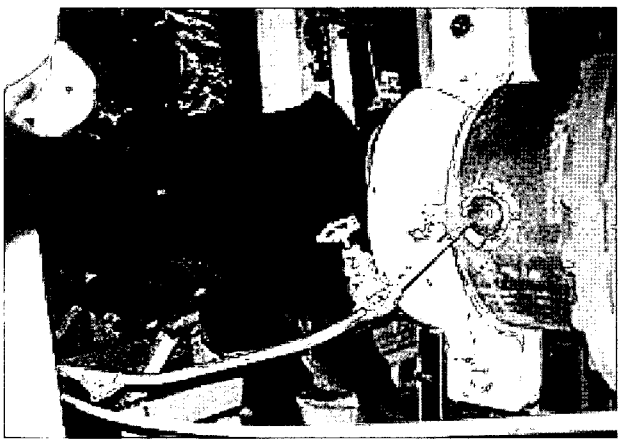

Fig. 2. A Recent Pipe Rupture Accident Occurred at the Position Just After a Flow Meter with an Orifice-typed Device, Reported in 2004 [3]

of carbon steel FAC on pH, usually in a pH range of up to about 9.5. The results show that carbon steel FAC usually decreases with an increasing pH [1-11].

In this study, to confirm whether FAC would decrease even in a pH range of over 9.5, and to confirm the effects of flow velocity, orifice distance, and material, we investigated the dependencies of FAC in single-phase, carbon steel (A106 Grade B) and low-alloy steels (1Cr-$\frac{1}{2}$Mo and 2$\frac{1}{4}$Cr-1Mo). The pH was maintained within a range from 8.0 to 10.0 with ammonia in an oxygen-free aqueous solution. The solution was re-circulated in an Erosion-Corrosion Test Loop under a flow velocity of 4 m/sec or 9 m/sec at 130°C for 500 hours.

2. MECHANISM OF FAC

Flow-accelerated corrosion is a process whereby the normally protective oxide layer on carbon or low-alloy steel dissolves into a stream of flowing water or a water-steam mixture. The FAC process occurs under both single and two-phase flow conditions. Because water is necessary to remove the oxide layer, FAC does not occur in lines transporting dry or superheated steam.

The FAC process is an extension of the generalized corrosion process of carbon steel in stagnant water. The major difference is the effect of the water flow at the oxide-solution interface. The FAC process can be divided into coupled processes that take into account the presence of the porous magnetite layer on the steel surface up to about 300°C [11].

The first process produces soluble ferrous ions at the oxide-water interface and this process can be separated into three simultaneous actions:
(1) metal oxidation occurs at the iron-magnetite interface in water with a reducing potential; (2) the ferrous species diffuse from the iron surface to the main water flow through the porous oxide layer; (3) the magnetite oxide layer at the oxide-water interface is dissolved by a reducing process, which is promoted by the presence of hydrogen.

The second process involves the transfer of the ferrous ions into the bulk water across the boundary layer. The concentration of ferrous ions in the bulk water is very low when compared to the concentration of ferrous ions at the oxide-solution interface. The corrosion rate increases if there is an increase of the water flow past the oxide-water interface.

This dissolution process is controlled by the oxidizing-reducing potential (ORP) of the water. In essence, the more reducing the feedwater is, the higher the dissolution and the level of the corrosion products measured in the feedwater are.

Under alkaline, deoxygenated (reducing) conditions, the primary reaction of the iron dissolution is inhibited by increasing the pH or by decreasing the reducing environment (i.e. ORP becoming more positive). This causes a reduction of the ferrous ion [Fe^{2+} and $Fe(OH)^{+}$] concentration.

The solubility of the ferrous hydroxide ($Fe(OH)_2$) rises with an increasing temperature to a maximum at around 150°C, then decreases with a steep drop to the solubility of the magnetite between 200 and 250°C [12].

3. EXPERIMENTAL PROCEDURE

3.1. Facility, Specimens, and Analyses

An Erosion-Corrosion Test Loop was designed and constructed, as shown in Fig. 3. Test specimens were made of carbon steel (A106 Grade B) and low-alloy steels [A336 P11$\frac{1}{2}$(1Cr- Mo) and A335 P22 (2$\frac{1}{4}$Cr-1Mo)], and their

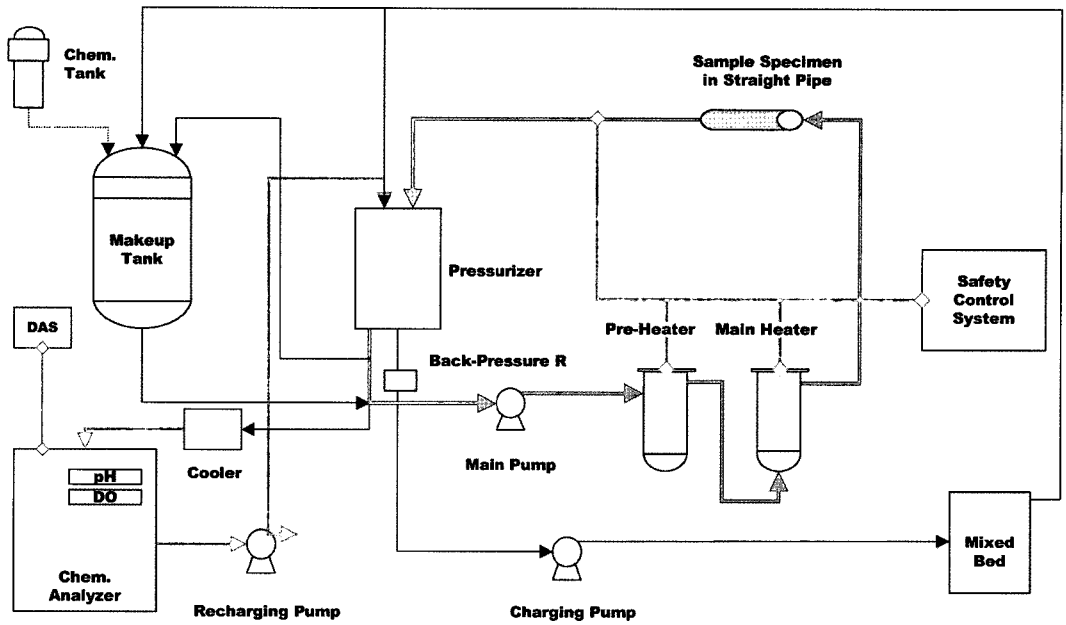

Fig. 3. Schematic Diagram of an Erosion-Corrosion Test Loop

Table 1. Chemical Composition of the Test Specimens

Mat.	Specification	Chemical Composition (Wt %)								
	(ASTM)	C	Mn	P	S	Si	Ni	Cr	Mo	Fe
1	A106 Gr. B	0.3	0.29~1.06	0.048	0.058	0.1				Balance
	(Commercial)	(0.15)	(0.64)	(0.003)	(0.014)	(0.19)	(0.06)	(0.03)	(0.01)	
2	A336 P11	0.15	0.3~0.6	0.03	0.03	0.5~1.0		1.0~1.5	0.44~0.65	Balance
	(1Cr-$\frac{1}{2}$Mo)	(0.1)	(0.36)	(0.009)	(0.009)	(0.56)		(1.06)	(0.48)	
3	A335 P22	0.15	0.3~0.6	0.03	0.03	0.5		1.9~2.6	0.87~1.13	Balance
	(2$\frac{1}{4}$Cr-1Mo)	(0.09)	(0.49)	(0.012)	(0.008)	(0.21)		(2.03)	(0.97)	

* Pipe: ID $\frac{1}{2}$", SCH 80 (~3.3 mm in wall thickness)
** Values in parentheses are the actual composition of product

chemical compositions are shown in Table 1.

Four ring-typed specimens, of which the inner surface (1.65 cm in inner diameter, 0.375 cm in width) only made contact with the stream, were positioned in a specimen bundle, as shown in Fig. 4. The four bundles were positioned at the specimen test section in the loop. Three of the bundles each contained an orifice with a 6-mm inner diameter for a velocity of 4 m/sec, while the fourth bundle had an orifice with a 4-mm inner diameter for a velocity of 9 m/sec.

Solution pH and dissolved oxygen (DO) content were measured by using an on-line pH-meter (Omega Co.) and an on-line DO-Analyzer (TOA Electrics Co.), respectively.

Surface characteristics of the specimens were observed and analyzed by using scanning electron microscopy (SEM) (JEOL JSM-6300 Scanning Microscope), x-ray diffraction (XRD) (Rigaku D/MAX-2000 X-ray Diffractometer), and x-ray proton spectroscopy (XPS) (XPS LAB MIC II, B.G. Scientific Co.). Dissolved iron concentrations sampled after 500 hours were analyzed by using an ICP-AES (Inductively Coupled Plasma–Atomic Emission Spectroscope,

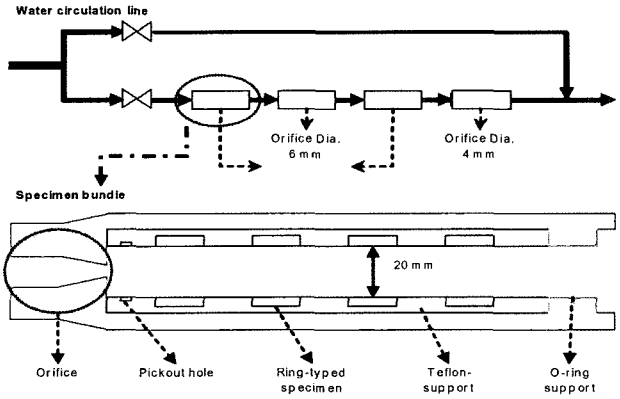

Fig. 4. Schematic Diagram of the Erosion-Corrosion Test Specimen

IRIS-DUO).

3.2. Experimental Methods

Before testing, the external impurities contaminated on the surface of the ring-typed specimens were ultrasonically cleaned, and the specimens were weighed after drying.

To obtain reasonable weight loss data within at least 500 hours, the experiment was carried out in a DO-free aqueous solution at 130°C, thus providing a maximum FAC rate for carbon steel and low-alloy steels.

The solution was de-aerated via a nitrogen gas injection and de-oxygenated via an oxygen-hydrazine reaction. The DO value detected by the on-line DO-meter located at the outlet of the stream passing the test section was maintained at less than 1 ppb, thus ensuring it was DO-free.

The pH-controlling agent used was ammonia, which is still widely applied to the secondary water chemistry systems of PWR nuclear power plants (NPPs). The solution pH values were kept at 8.0, 8.5, 9.0, 9.3, 9.43, 9.5, 9.625, 9.75, and 10.0.

We observed and analyzed the surface characteristics and chemical features of the specimens before and after 500 hours, using SEM, XPS, and XRD; in addition, ICP-AES was used to measure the concentration of iron in a given solution.

4. RESULTS AND DISCUSSION

4.1. Characteristics of the Oxide Layer on the Carbon Steel Specimens

Figure 5 shows SEM micrographs of carbon steel after 500 hours at pH 9.0, under a flow velocity of 4 m/sec, at 20.4 mm from the orifice, in the oxygen-free aqueous solution at 130°C The non-tested surface is also shown. Usually, general corrosion is accompanied by a lower energy transfer rather than by mechanical damage, and

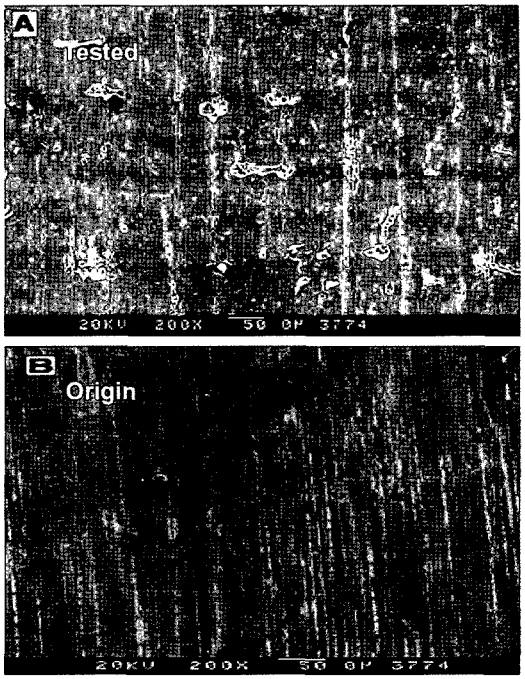

Fig. 5. SEM Micrographs of Carbon steel (CS) after 500 Hours at pH 9.0 at the Flow Velocity of 4 m/sec (A), and the As-received Surface (B)

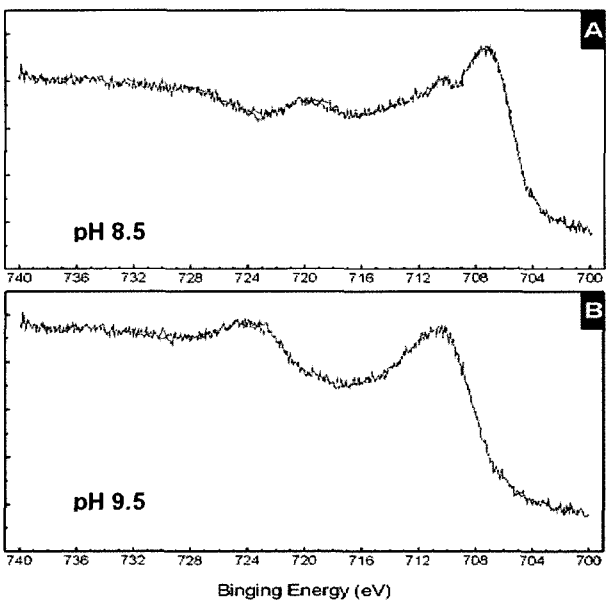

Fig. 6. Fe_{2p} XPS Spectrum of Fe_3O_4 Formed on the Carbon Steel (CS) After 500 Hours at pH 8.5 (A) and 9.5 Under the Flow Velocity of 4 m/sec

FAC generally results in traces, such as grooves, ripples, gullies, or thin pitting forms [2]. In this study, the tested specimen showed mainly grooves that formed due to the

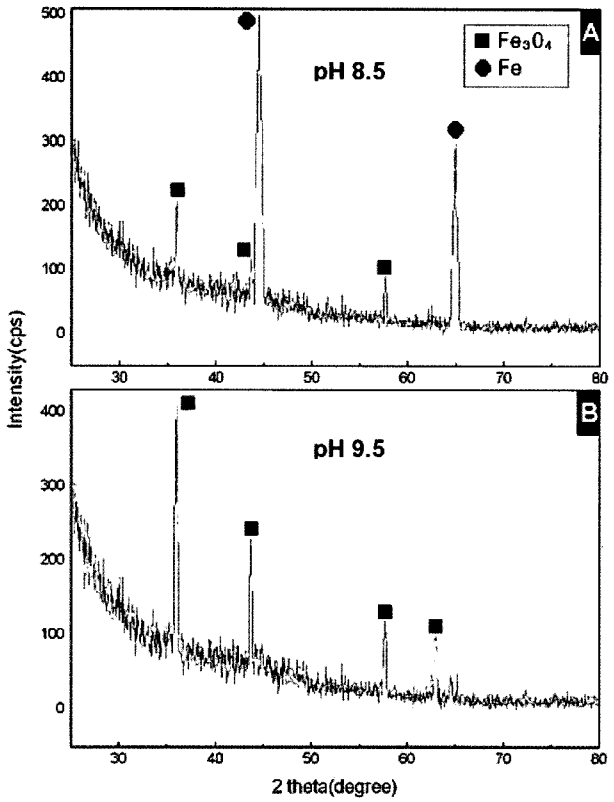

Fig. 7. XRD Patterns of the Carbon Steel at pH 8.50 (A) and 9.50 (B) at 130°C Under the Flow Velocity of 4 m/sec

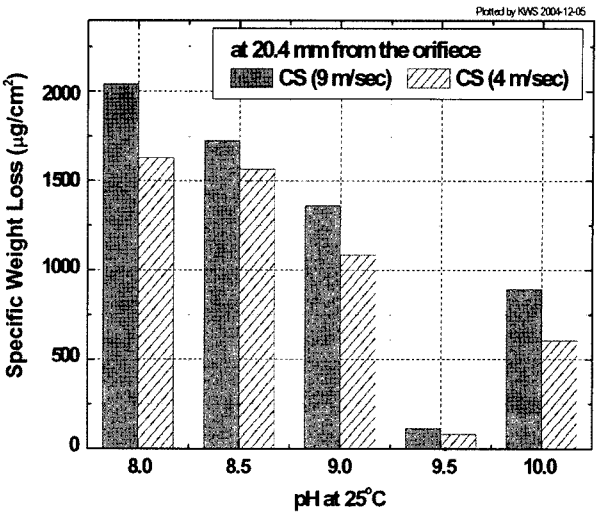

Fig. 8. Weight Loss of the Carbon Steel After 500 Hours at 20.4 mm from the Orifice, Dependent Under the Flow Velocities of 4 and 9 m/sec

fluid flow from left to right. The low-alloy steel specimens showed features similar to those of the carbon steel.

Figure 6 shows Fe_{2p} XPS spectra of Fe_3O_4 formed on the carbon steel specimens after 500 hours at pH 8.5 and 9.5, under a flow velocity of 4 m/sec, at 20.4 mm from the orifice, at 130°C The Fe_{2p} XPS spectrum revealed the chara-cteristic peak of Fe_3O_4 at a binding energy of 710.4 eV, and the characteristic peak of Fe at 707.0 eV. These peaks showed that the surface of the carbon steel specimen obtained at pH 8.5 contained less magnetite and more iron than those obtained at pH 9.5.

This tendency was also confirmed by the XRD patterns of the carbon steel specimen at pH 8.5 and at pH 9.5, as shown in Fig. 7. Two strong peaks of Fe at 2Θ degree of 44.5 and 65.0, including another four weak peaks of Fe_3O_4 at the rest peaks marked in this figure, appeared to be higher for the specimen obtained at pH 8.5 than at pH 9.5.

This means that the magnetite dissolution rate at pH 8.5 was higher than that at pH 9.5, showing the dependency of carbon steel FAC on pH and magnetite solubility [12].

4.2 Effect of Flow Velocity on Weight Loss of Carbon Steel

Figure 8 shows the weight loss of carbon steel specimens after 500 hours, under flow velocities of 4 and 9 m/sec, at 20.4 mm from the orifice, at 130°C, and in the pH range of 8.0~10.0.

There is a flow velocity dependency of weight loss due to the FAC on the carbon steel. The weight loss obtained at a flow velocity of 9 m/sec is approximately 30% higher than that obtained under 4 m/sec. A significant decrease in weight loss of carbon steel at pH 9.5 can be explained by the solubility of iron oxide as a function of pH, as described below.

4.3. Effect of pH on Weight Loss of Carbon Steel and Low-Alloy Steels

As shown in Fig. 9, the weight loss of specimens of carbon steel and low-alloy steels (P11: 1Cr-$\frac{1}{2}$Mo, P22: 2 $\frac{1}{4}$Cr-1Mo) after 500 hours, at a pH of 8.0~10.0, under a flow velocity of 4 m/sec and 9 m/sec, at 20.4 mm from the orifice, and at 130°C is dependent on the pH and material.

The weight loss appeared to decrease with an increase of pH to a range of 8.0~9.5. In contrast, for a pH range of 9.5~ 10.0, the weight loss inversely increased, showing a minimum at a pH of about 9.5.

The most commonly accepted mechanism of FAC in carbon steel and low-alloy steels in deoxygenated water flowing at a high flow rate and with a high temperature is that chemically reductive dissolution of the magnetite (Fe_3O_4) film occurs by an enhanced mass transport of the soluble iron species.

To confirm the magnetite solubility effect on the experimental weight loss, the concentrations of the soluble iron species dissolved from magnetite, such as Fe^{2+}, $FeOH^+$, $Fe(OH)_{2aq}$, $HFeO_2^-$, FeO_2^{2-} and $H_2FeO_3^-$, and the total

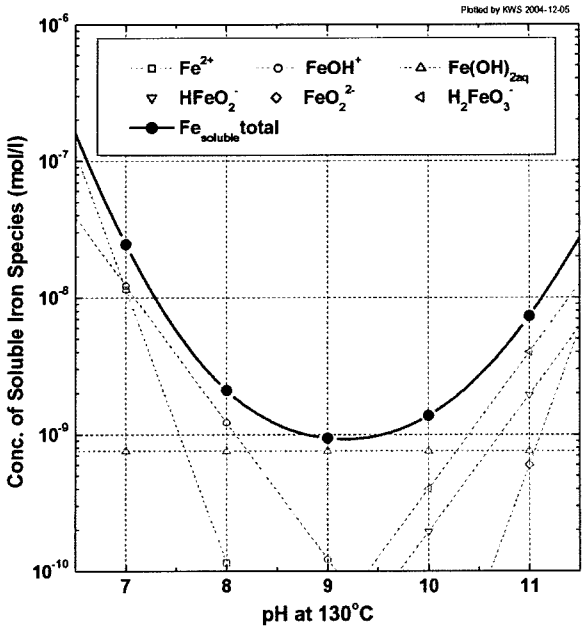

Fig. 9. Contributions of the Individual Soluble iron Species to the Total Magnetite Solubility in an Aqueous Solution, Calculated at 130°C, Dependent on pH

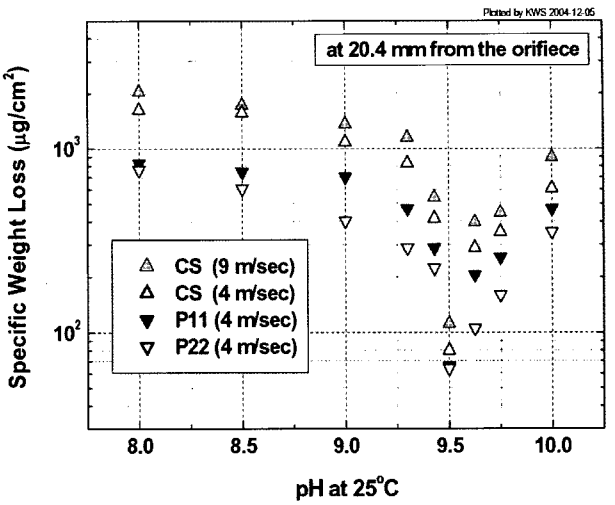

Fig. 10. Weight Loss of the Specimens of Carbon Steel (CS) and Low-alloy Steels (P11: 1Cr-½Mo, P22: 2¼Cr-1Mo) at 20.4 mm from the Orifice, Dependent on the pH and Material at 130°C After 500 Hours

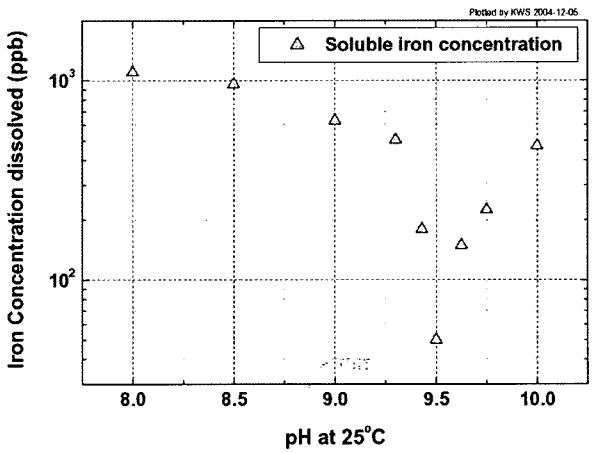

Fig. 11. Dissolved Iron Concentration in the Aqueous Solution of the Test Loop at pH 8~10 After 500 Hour-testing

soluble iron, were thermodynamically calculated at 130°C For the calculation, the following reactions were used with the thermodynamic values obtained from literature [12]:

$$Fe_3O_4 + 2H^+ = 2FeOOH + Fe^{2+} \quad (1)$$

$$Fe_3O_4 + H^+ + H_2O = 2FeOOH + FeOH^+ \quad (2)$$

$$Fe_3O_4 + 2H_2O = 2FeOOH + Fe(OH)_{2aq} \quad (3)$$

$$Fe_3O_4 + 2H_2O = 2FeOOH + HFeO_2^- + H^+ \quad (4)$$

$$Fe_3O_4 + 2H_2O = 2FeOOH + FeO_2^{2-} + 2H^+ \quad (5)$$

$$Fe_3O_4 + H_2O = H_2FeO_3^- + H^+ \quad (6)$$

The calculated results are plotted in Fig. 10. In the pH range of 8.0~9.5, the reactions that predominantly contributed to the total soluble iron concentration at 130°C were shown to be the reactions of (1), (2), and (3). While, in the pH range of 9.5~10.0, the reactions of (4), (5), and (6) were the predominant contributors.

The pH dependency of the magnetite dissolution obtained from the calculation seemed to be consistent with the experimental weight loss results and with the soluble iron concentration experimentally obtained by ICP-AES, as shown in Fig. 11.

This means that, under these experimental conditions, the FAC of the carbon steel and the low-alloy steels depended on the magnetite solubility.

There are very few references in the literature regarding the effect of pH on the FAC of carbon steel and low-alloy steels. Water chemistry personnel at NPPs should carefully consider this pH dependency and control water system pH levels to enable mitigation of piping material FAC.

4.4 Effect of Orifice Distance on Weight Loss of Carbon Steel and Low-Alloy Steels

In this experiment, specimens of carbon steel and low-alloy steels were laid out at positions of 6.8, 13.6, 20.4, and 27.2 mm from the orifice in a specimen bundle, as shown in Fig. 4. In Fig. 12 are plotted the weight losses of carbon steel and P11 and P22 steels as a function of pH and distance from the orifice. A clear dependency of FAC on

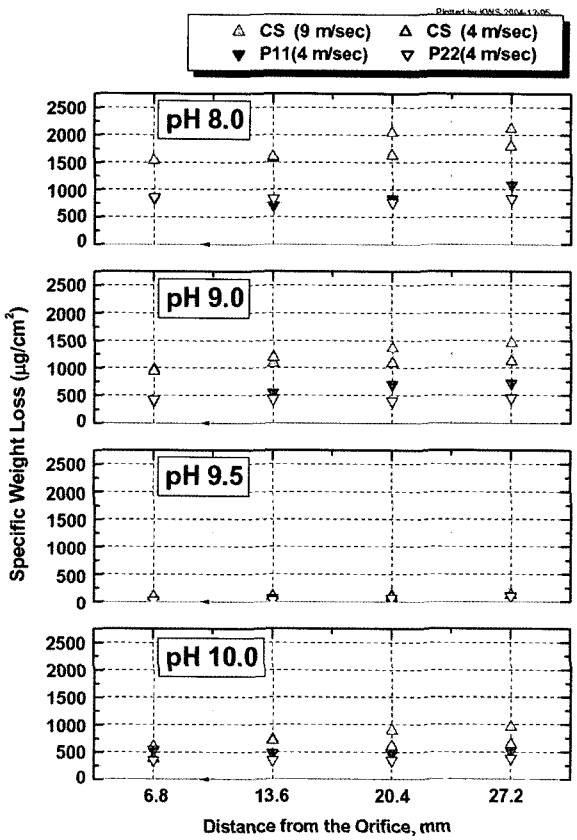

Fig. 12. Weight Loss of the Specimens of Carbon Steel (CS) and Low-alloy Steels (P11 and P22) at pH 8.0, 9.0, 9.5 and 10.0, Dependent on the Materials at 130°C After 500 Hours, Versus the Distance from the Orifice

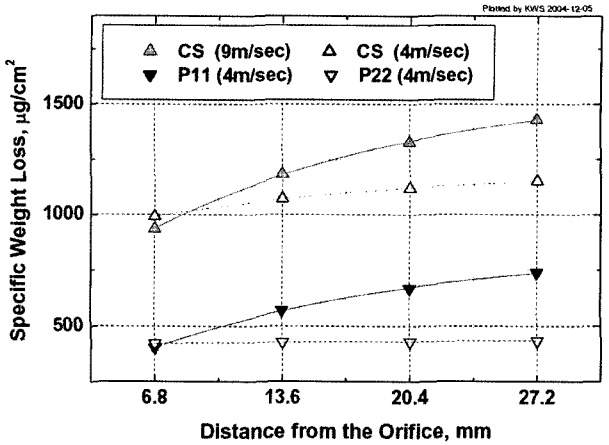

Fig. 13. Regression Curves of the Weight Loss of CS, P11 and P22 After 500 Hours at pH 9.0 and 130°C as a Function of Orifice Distance

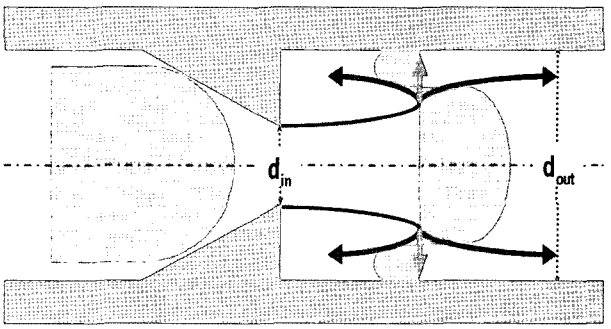

Fig. 14. Turbulent Pipe with Separation (complex velocity field with reverse flow)

pH and distance is observed.

The orifice distance dependency was re-plotted at pH 9.0 after a regression, as shown in Fig. 13. The weight losses of the carbon steel and the P11 specimens increased with increases in the distance of the specimen from the orifice. The P22 specimens did not show any orifice distance dependency.

This phenomenon was thought to be due to the laminar and turbulent flow that is generated just after passing the orifice, forming a complex velocity with a reverse flow, as shown in Fig. 14. In other words, a pipe would be more damaged by a FAC at a certain distance from the orifice, and at high flow velocity, than at other locations.

To prevent the kind of pipe rupture shown in Fig. 2, the surface, thickness, and material of a given piping system located at certain plant-specific distance from an orifice must be reconsidered.

4.5 Effect of Material on Weight Loss of Carbon Steel and Low-Alloy Steels

Figure 13 shows the effect of material on the weight loss of the specimens. This figure also shows that the weight losses of carbon steel specimens, at flow velocities of 9 and 4 m/sec, and those of the P11 specimens, at a flow velocity of 4 m/sec, were shown to be greater than that of the P22 specimens at 20.4 mm from the orifice.

This material dependency of the weight loss is also shown in Fig. 15. This figure shows the Cr_{2p} XPS spectra in Cr_2O_3 formed on the surfaces of the specimens of carbon steel and low-alloy steels (P11 and P22) after 500 hours at pH 9.75 at a flow velocity of 4 m/sec. It was found that the steels containing more chromium (P11 and P22) exhibited approximately half the weight loss of that of carbon steel.

Furthermore, as shown in Fig. 16, the XRD patterns of the carbon steel showed three strong peaks of Fe_3O_4 at 2Θ degrees of 36.0, 43.5, and 57.5, but no peaks of Cr_2O_3. While, the P11 and the P22 showed strong peaks of Cr_2O_3 at a 2Θ degree of 33.0, including some weak peaks of Fe_3O_4, suggesting the coexistence of both Fe_3O_4 and Cr_2O_3.

The chromium contained in the molecular matrix of the specimens of the P11 (1Cr-½Mo) and P22 (2¼ Cr-1Mo)

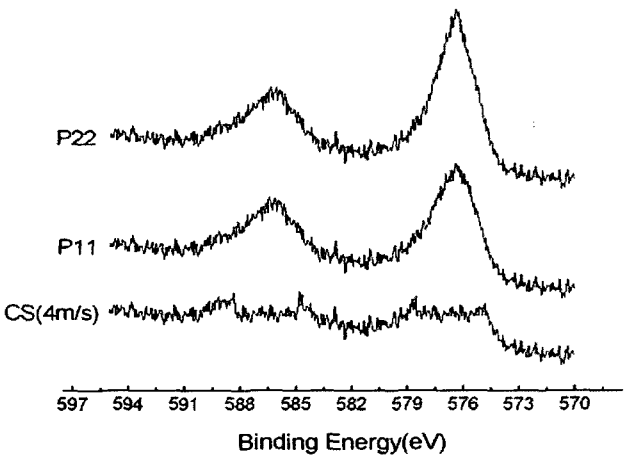

Fig. 15. Cr_{2p} XPS Spectrum in Cr_2O_3 Formed on Carbon Steel and Low-alloy Steels (P11 and P22) After 500 Hours at pH 9.75 Under the Flow Velocity of 4 m/sec

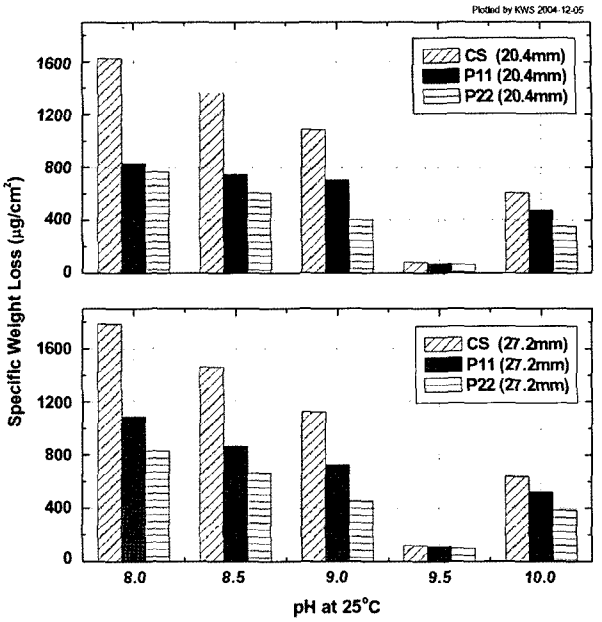

Fig. 17. Weight Loss of Specimens of CS, P11 and P22 After 500 Hours at 20.4 and 27.2 mm from the Orifice and 130°C, Showing Dependence on the Material

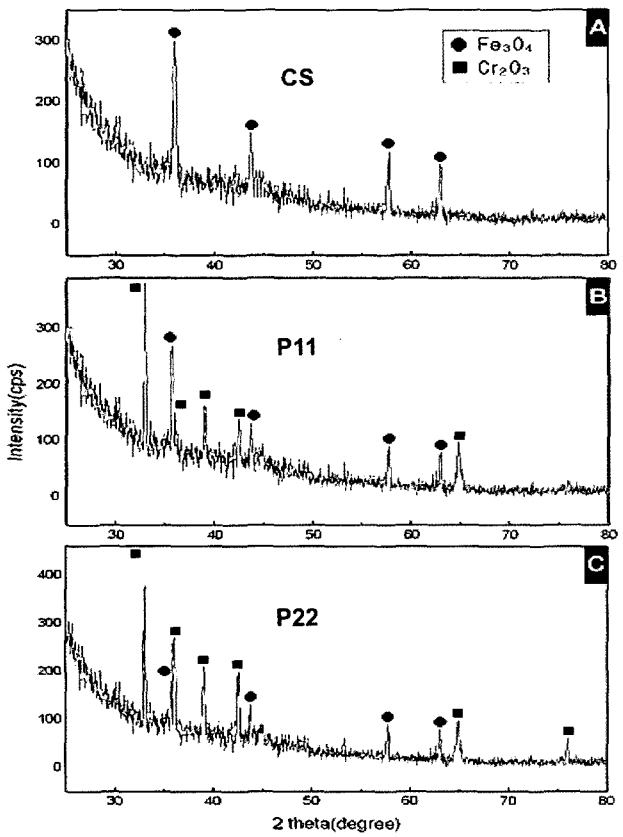

Fig. 16. X-ray Diffraction Patterns of Carbon Steel (A), P11 (B) and P22 (C) After 500 Hours at pH 9.75 and 130°C Under the Flow Velocity of 4 m/sec

was thought to be formed as a non-stoichiometric spinel, $Fe_xCr_yFe_{2-x-y}O_4$, with a very high stability due to its extremely low solubility in the high temperature aqueous solution. In other words, the VI-B transition elements, such as Cr (and Mo) added into the carbon steel matrix gave excellent resistance against FAC - approximately two times higher than that of the original one - at a low alkaline pH, as shown in Fig. 17.

To compare carbon steel and low alloy steel resistances to FAC, the values of the coefficient and the constant of a linear weight loss-pH equation was regressed as the following:

$$WL_{regressed} = A \times pH + B \quad (7)$$

Here, $WL_{regressed}$ is the regressed weight loss, A is the coefficient of the pH dependence, and B is the constant of the linearly regressed equation. The values are presented in Table 2, and plotted in Fig. 18. In the range of pH from 8.0 to 9.5 and from 9.5 to 10.0, respectively, the values of A and B were shown to be distinguishably different, depending on the materials. The values of A and B might suggest that an index of the pH and material dependency of carbon steel and low-alloy steel FAC would illustrate sensitivity to FAC.

Based on this material dependency, it was thought to be desirable to alternate the material composition of the secondary piping system of NPPs, using that of low-alloy

Table 2. The Constant Values of WL (Regressed weight loss ($\mu g/cm^2$)) = A x pH + B for Linear Curve Fitting

Material	WL (Regressed weight loss ($\mu g/cm^2$)) = A × pH + B			
	pH 8.0~9.5		pH 9.5~10	
	A	B	A	B
CS 9m/s	-1,190	11,770	1,265	-11,793
CS 4m/s	-1,013	9,973	838	-7,785
P11 4m/s	-473	4,732	670	-6,242
P22 4m/s	-455	4,446	525	-4,924

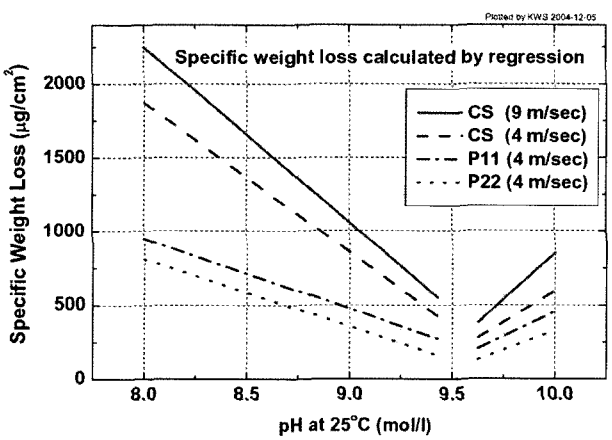

Fig. 18. Regression Curves of the Weight Loss of CS, P11 and P22 at 20.4 mm from the Orifice at 130°C, Showing Dependence on the Material

steels, such as 2¼Cr-1Mo. This could be done when a secondary piping system material is designed for new NPP construction and, particularly, when an old piping system has to be replaced after an accident.

5. CONCLUSION

To investigate the dependency of the FAC of carbon steel and low-alloy steels [P11 (1Cr-½Mo) and P22 (2¼Cr-1Mo)] on pH levels, orifice distances, and materials, experiments were carried out using flow velocities of 4 m/sec and 9 m/sec in a pH range of 8.0~10.0 in a dissolved oxygen-free aqueous solution re-circulated in an Erosion-Corrosion Test Loop at 130°C for 500 hours. The following observations were made:

The weight loss of carbon steel appeared to increase with an increase of flow velocity.

The weight loss of the carbon and low-alloy steel specimens was shown to be distinguishably dependent on the pH level. In a pH range from 8.0 to 9.5, weight loss decreased; however, it increased in a pH range from 9.5 to 10.0. Thus, NPP personnel should carefully control the system water pH to better mitigate FAC.

The weight losses of carbon and low-alloy steel specimens located further from the orifice were shown to increase within a distance range from 6.8 to 27.2 mm. To prevent possible piping ruptures, it is recommended that the surface, thickness, and material of a given piping system located at a certain plant-specific distance from an orifice be carefully reconsidered.

This study also showed that low alloy steels have twice the resistance against FAC than that of carbon steel. Therefore, it is advisable to alternate the composition of the secondary piping system material of the NPPs, using low-alloy steels, such as 2¼Cr-1Mo, particularly when old system pipes have to be replaced.

Acknowledgements

This work has been carried out under the nuclear research and development program of the Ministry of Science and Technology of Korea.

REFERENCES

[1] Shah, "Flow-Accelerated Corrosion of PWR Carbon Steel Components", *Symposium on Life Extension and Aging Management of Nuclear Power Plant Components in Korea*, Korea Institute of Nuclear Safety, Taejon, Korea, July (1999)

[2] Kunze and J. Nowak, "*Erosion Corrosion Damage in Steam Boiler*", Werkstoffe und Korrosion, 33, pp. 262~273 (1982)

[3] "Accident at the Kansai Electric's Mihama-3 NPS", JAIF Focus, Japan Atomic Industrial Forum, Inc., August 10, 2004

[4] Marta U. Gmurczyk, Aaron Barkatt, David Ballard, Galina Cherepakhov, William Kessler and Reynolds Burns, "Identification of corrosion modes in steam pipes from the secondary system at Indian Point 2", *Corrosion 98*, paper No. 130, National Association for Corrosion Engineers, Houston, TX (1998)

[5] M. J. Moore and C. H. Sieverding, "*Two-Phase Steam Flow in Turbines and Separators*", Chapter 6, Hemisphere Pub. Corp. (1976)

[6] G. A. Delp, J. D. Robison and M. T. Dedlack, "Erosion/Corrosion in Nuclear Plant Steam Piping: Causes and Inspection program Guidelines", NP-3944, Electric Power Research Institute, Palo Alto, CA (1985)

[7] N. S. Hirota, "*Erosion-Corrosion in Wet Steam Flow*", in Metals Handbook. 9th ed., Vol.13 - Corrosion, ASM International, Metals park, OH p. 964-971 (1987)
[8] B. Chexal, J. Horowitz, R. Jones, B. Dooley, C. Wood, M. Bouchacourt, M., F. Remy, F. Nordmann, P. St. Paul, "Flow-Accelerated Corrosion in Power Plants", TR-106611, Electric Power Research institute, PaloAlto, CA (1996)
[9] H. Keller, VGB, Kraftwerkstechnik, 54, No.5, 292, 1974
[10] M. Izumia, A. Minato, F. Hataya, K. Ohsumi, Y. Ohshima and S. Ueda, "Corrosion and/or Erosion in BWR Plants and Their Countermeasures", Water Chemistry and Corrosion Products in Nuclear Power Plants, International Atomic Energy Agency, Vienna, Austria, p. 61 (1983)
[11] R. B. Dooley and V. K. Chexal, "*Flow-accelerated corrosion of pressure vessels in fossil plants*", International Journal of Pressure Vessels and Piping, Volume 77, Issues 2-3, February 2000, p. 85-90 (2000)
[12] G. Bohnsack, "*The Solubility of Magnetite in Water and in Aqueous Solutions of Acid and Alkali*", Chapter 10, Published by Vulkan-Verlag, Essen, Germany (1987)